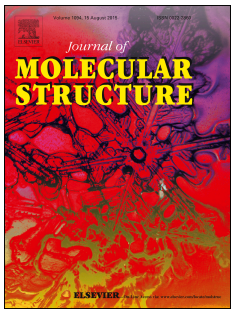

Synthesis and structural characterization of phosphinate coordination polymers with tin(IV) and copper(II)

Khodayar Gholivand, Nasrin Fallah, Ali Asghar Ebrahimi Valmoozi, Akram Gholami, Michal Dusek, Vaclav Eigner, Mahsa Pooyan, Fahimeh Mohammadpanah

PII: S0022-2860(19)31478-4

DOI: https://doi.org/10.1016/j.molstruc.2019.127369

Reference: MOLSTR 127369

To appear in: *Journal of Molecular Structure*

Received Date: 13 April 2019

Revised Date: 16 October 2019

Accepted Date: 5 November 2019

Please cite this article as: K. Gholivand, N. Fallah, A.A. Ebrahimi Valmoozi, A. Gholami, M. Dusek, V. Eigner, M. Pooyan, F. Mohammadpanah, Synthesis and structural characterization of phosphinate coordination polymers with tin(IV) and copper(II), *Journal of Molecular Structure* (2019), doi: https://doi.org/10.1016/j.molstruc.2019.127369.

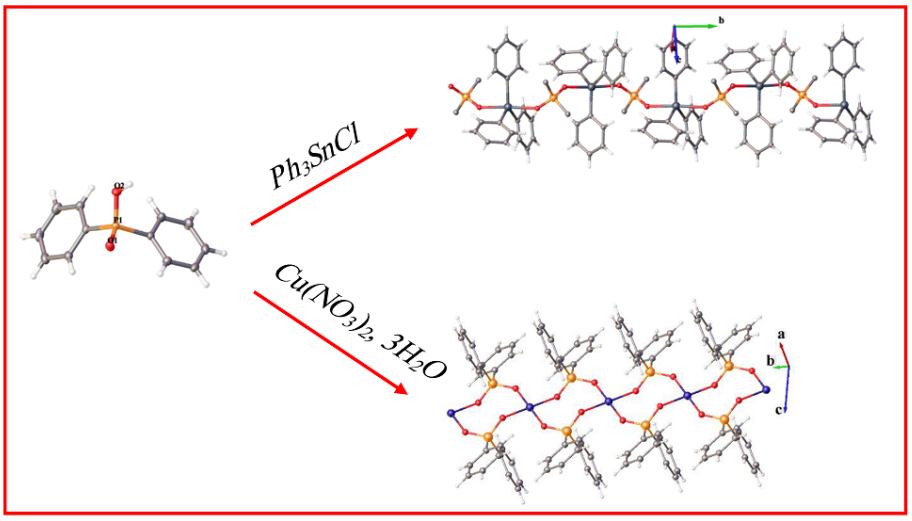

Synthesis and structural characterization of phosphinate coordination polymers with tin(IV) and copper(II)

Khodayar Gholivand[a, *], Nasrin Fallah[b], Ali Asghar Ebrahimi Valmoozi[a], Akram Gholami[a], Michal Dusek[c], Vaclav Eigner[c], Mahsa Pooyan[a], Fahimeh Mohammadpanah[a]

[a]*Department of Chemistry, Faculty of Basic Sciences, TarbiatModares University, Tehran, Iran.*
[b]*Department of Chemistry, Science and Research Branch, Islamic Azad University, Tehran, Iran.*
[c]*Institute of Physics ASCR, Na Slovance 2, 182 21 Prague 8, Czech Republic.*

Abstract

In this work, we report the synthesis and X–ray characterization of diphenylphosphinic acid (***L***) (redetermination at 100 K), and its two polymeric phosphinate complexes; $[(C_6H_5)_2P(O)OSn(C_6H_5)_3]_n$ (***C1***) and $[Cu(O_2PPh_2)_2]_n$ (***C2***), resulted from the bidentate coordinatioan of ***L***. Sn(IV) centers in ***C1*** are five-coordinate in a distorted trigonal bipyramidal geometry. One dimensional coordination chains of ***C2*** are made by double-bridging ligands between the copper atoms, surrounded with four P-O in a square planar polyhedron. Structural characterization of the complexes revealed that M-O bonds are responsible for the assembly of the primary structural motifs in both the complexes while C–H…π and H…H interactions are effective in organizing these molecules into extended 3D architectures. The quantitative mapping of interactions was also analyzed using Hirshfeld surface analysis. With respect to the ^{31}PNMR spectra, there are probably fast transformations in the solution and different types of coordinated and dissociated species are in balance, consistent with the optimized structures in the solvent and gas phases.

Keywords: Coordination polymer; Phosphinate; Tin(IV); Copper(II); Intermolecular interactions; Hirshfeld surface analysis.

1. Introduction

In the last decades, the structural diversity of coordination polymers, as this type of materials makes them attractive for a variety of potential applications that contain optics, small-molecule storage, and separation science [1-3]. The apparently limitless combination of metal ions and organic molecules have created a massive array of structural topologies. In order to identify the full potential of this exciting field, extensions to a variety of organic molecules have been explored. Phosphonates are one of the things that have attracted a lot of attention.

phosphonates have been used for vigorous crystalline materials that are capable of being characterized by single-crystal X-ray diffraction. Challenges with phosphonates, as a class of organic molecules, historically have included quick precipitation due to the formation of densely layered phases which frequently form intractable solids that are problematic to characterize [4]. Additionally, compared to other organic compounds such as carboxylates, phosphonates offer much more bridging modes to metals, making the formation of structural motifs for the design of specific materials less predictable. Our interest lies in exploring phosphinates ($Ar_2PO_2^-$) as less conventional organic linker molecules that could be useful in the synthesis of coordination polymers.

In this research, diphenylphosphinic acid (***L***) has been used in the reaction with $SnPh_3Cl$ and $Cu(NO_3)_2$, $3H_2O$. This ligand bears the close resemblance to Benzoic acid, and it seems interesting to compare the pattern and strength of hydrogen bonding and to study the packing in these two structures. Crystal structures of many complexes of carboxylate ligands with tin and copper compounds have been reported, and in some cases, their anticancer and antibacterial properties have been investigated [5-9]. It is expected that by replacing these ligands with phosphates, new and different structures are obtained which can affect the properties and activities of the complex.

In this regard, structural studies of ligand ***L*** and two new coordination polymers with the formula $[(C_6H_5)_2P(O)OSn(C_6H_5)_3]_n$ (***C1***) and $[Cu(O_2PPh_2)_2]_n$ (***C2***) in the solid form were carried out using crystallography and the main noncovalent intermolecular interactions were elucidated by Hirshfeld surface analysis. The chemical behavior and stability of ***C1*** and ***C2***, in comparison with other synthetized complexes, were investigated.

2. Experimental

2.1. Chemicals and Characterizations

Triphenyltin chloride and copper (II) nitrate trihydrate used in this study were purchased from Merck, and diphenylphosphinic chloride (98%) from Acros Organics chemical company and used without further purification. Solvents were purified and dried following the standard procedures. Melting point was obtained with an Electrothermal instrument. Infrared spectra were recorded in KBr discs in the region 4000–400 cm^{-1} on a Thermo Nicolet NEXUS 870 FT-IR spectrometer. The FT-Raman spectrum (in the range 3600-100 cm^{-1}) was measured on a NICOLET 960-ESP FT-RAMAN spectrometer equipped with a liquid nitrogen cooled germanium detector and a Diode-pumped solid state laser (emitting radiation at a wavelength of 1064 nm). The spectrum was recorded at a resolution of 2 cm^{-1}. NMR spectra were recorded on a Bruker Avance DRX500 spectrometer. ^{1}H chemical shifts was measured relative to internal TMS. ^{31}P and ^{119}Sn chemical shifts were determined relative to 85% H_3PO_4 and $Sn(CH_3)_4$ as external standards, respectively.

X-ray data were collected on a Bruker APEX II CCD area detector [10] with graphite monochromated Mo Ka radiation (λ = 0.71073 Å). The structure was refined with SHELXL 97 [11] by full-matrix leastsquares on F2. The positions of hydrogen atoms were obtained from the difference Fourier map. The CIF files have been deposited with the CCDC and have been given the deposition numbers 1861944, 1846819 and 1835509 for ***L***, ***C1*** and ***C2***, respectively. Crystal data and experimental details of the structure determination for compound ***L***, ***C1*** and ***C2*** are listed in Table 1 of Supporting Information

2.2. Synthesis of ligand

$(C_6H_5)_2P(O)OH$ (*L*)

Diphenylphosphinic acid was synthesized by the reaction of 2 mmol (0.473g) of $(C_6H_5)_2P(O)Cl$ and 2 mmol (0.04g) of H_2O in CH_2Cl_2 at room temperature. After stirring for 4 h, the solvent was evaporated, and the residue was washed with cold water and dried. A white solid resulted in a yield of 90%. Suitable single crystals of ***L*** were obtained by a slow

evaporation method using methanol/ dichloromethane solvents mixture. Physical and spectroscopic data of ***L*** are presented below. $(C_6H_5)_2P(O)OH$ (***L***). Yield: 90%; m.p. 194-196 C, Selected IR data (KBr, cm^{-1}):3429 s (υO-H), 1639 s (υC=C), 1433 s (υP-C), 1184 s (υP=O), 1120 s, 968 s. Selected Raman data: 3352, 1593, 1307, 1273, 202. ^{31}P NMR ($CDCl_3$, ppm): δ= 24.2. ^{1}H NMR (DMSO-*d6*, ppm): δ= 7.47 (m, 6H, 2Ph), 7.71 (m, 4H, 2Ph). ^{31}P NMR (DMSO-*d6*, ppm): δ= 23.4.

2.3. Synthesis of complexes

$[(C_6H_5)_2P(O)OSn(C_6H_5)_3]_n$ (*C1*)

A solution of triphenyl tin chloride (0.038 g, 0.01 mmol) in 10 ml chloroform was added to the 10 ml solution of ***L*** (0.022 g, 0.01 mmol) in chloroform. The resulting mixture was stirred at room temperature for 2 days. Single crystals of ***C1*** were obtained by slow evaporation of the solvents. Yield: 86%; m.p. 225-227°C, Selected IR data (KBr, cm^{-1}): 3058 m,1652 m (υC=C), 1427 m (υP-C), 1128 s (υP=O), Selected Raman data: 3357, 1593, 1342, 1290, 123, ^{1}H NMR ($CDCl_3$, ppm): δ= 7.45 (m, 12H, 2Ph+Ph_3Sn), 7.70 (m, 6H, O-Ph_3Sn), 7.80 (m, 4H, 2Ph). ^{31}P NMR ($CDCl_3$, ppm): δ=24.4, 33.4.

$[Cu(O_2PPh_2)_2]_n$, (*C2*)

To a methanolic solution of $Cu(NO_3)_3$.$3H_2O$ (1.0 mmol in 10 ml methanol), a solution of ***L*** (1.0 mmol in 10 ml acetonitrile) was added under stirring. The stirring was continued for 2 days. Single crystals of ***C2*** were obtained by slow evaporation of the solvents. Single crystals were filtered, washed with n-hexane and dried. Yield: 78%; m.p. 308-310°C, Selected IR data (KBr, cm^{-1}): 1437 m (υP-C), 1128 s (υP=O), 1051 s, 692, Selected Raman data: 3097, 1595, 1383, 1383, 1298, 1219, 166. ^{1}H NMR (DMSO-*d6*, ppm): δ= 7.35-7.64 (m, 2Ph). ^{31}P NMR (DMSO-*d6*, ppm): δ= 23.2, 34.6.

Changing the stoichiometric ratio to 1: 0.5 (ligand: metal) also leads to the formation of the same complexes. The synthesis pathway of compounds ***L***, ***C1*** and ***C2*** was represented in **Scheme 1**

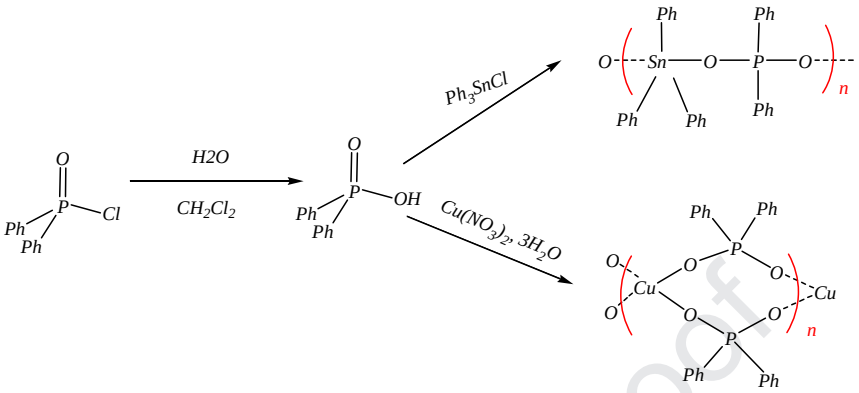

Scheme 1. Synthesis pathway of ***L***, ***C1*** and ***C2***.

Table 1 Single crystal data collection and refinement for ***L, C1*** and ***C2*.**

Parameters	***L***	***C1***	***C2***
Empirical formula	$C_{12}H_{11}O_2P$	$C_{30}H_{25}O_2PSn$	$C_{24}H_{20}Cu_1O_4P_2$
Formula weight	218.18	567.16	497.9
Temperature (K)	100(2)	100(2)	120
Wavelength (Å)	0.71073	0.71073	0.71073
Crystal system	Monoclinic	Monoclinic	Monoclinic
space group	$P2_1/c$	*P21/n*	*C12/c1*
a (Å) *b* (Å) *c* (Å) *α* (°) *β* (°) *γ* (°)	11.4612(10) 5.9559(5) 15.6442(13) 90 100.2093(16) 90	13.7991(4) 12.3203(4) 14.7297(5) 90 96.8640(10) 90	16.5181(8) 5.0529(3) 25.4454(13) 90 96.231(4) 90
V (Å^3)	1050.99(15)	2486.23(14)	2111.2(2)
Z, Calculated density (Mg.m^{-3})	4, 1.379	4, 1.515	4, 1.566
Absorption coefficient (mm^{-1})	0.236	1.117	1.219
F(000)	456	1144	1020.0
Crystal size (mm)	0.21×0.18×0.17	0.30×0.22×0.20	0.339×0.131×0.051
θ range for data collection (°)	1.81-29.00	1.91-30.00	3.85-29.47
Limiting indices	-15<=h<=15 -8<=k<=8 -21<=l<=21	-19<=h<=19 -17<=k<=17 -20<=l<=2	-20<=h<=21 -6<=k<=6 -30<=l<=33
Reflections collected / unique	12304./.2793 [R(int)=0.0335]	31919./.7243 [R(int) =0.0283]	12362./.2640 [R(int) =0.0265]
Completeness to theta	100.0 %	100.0 %	98%
Absorption correction	Semi-empirical from equivalents	Semi-empirical from equivalents	analytical
Max.andmin.transmission	0.961 and 0.952	0.807.and.0.730	0.942 and 0.804
Refinement method	Full-matrix least-squares on F2	Full-matrix least-squares on F2	Full-matrix least-squares on F2

Data/restraints/parameters	2793 / 0 / 140	7243 / 0 / 307	2640 / 0 / 108
Goodness-of-fit on F^2	1.041	1.001	2.02
Final R indices	R1=0.0338, wR2 = 0.0924	R1=0.0201, wR2 = 0.0470	R1= 0.0432, wR2 = 0.1270
R indices (all data)	R1=.0.0438, wR2= 0.1000	R1= 0.0258, wR2= 0.0493	R1= 0.0530, wR2= 0.1314
Largest diff. peak and hole (e.Å-3)	0.504 and -0.344	0.419 and -0.315	0.56 and -0.58

2.4.Computational details

The computations were performed with the Gaussian 09 set of programs [12]. Full optimization of the molecular geometry of ***L***, ***C1*** and ***C2*** has been made .The theoretical studies have been performed by density functional methods: B3LYP, which is the widely used three parameter hybrid functional [13]. We employed the LanL2DZ effective core potential and basis set for tin and copper [14] and the 6-311G(d) basis set for the remaining atoms(C, H, O and P) of ***C1*** and ***C2***

3 Results and discussion

3.1 Spectroscopic studies

The spectrum of ***L*** shows a broad band centered around 3429 cm^{-1} assignable to υ−str(O–H) vibration, whereas in ***C1*** and ***C2***, this signal is completely removed, indicating the connection of oxygen to the metal. The P=O stretching vibrations were observed at 1184 and 1120 cm^{-1} in ***L*** which shift to 1128 and 1062 cm^{-1}in ***C1*** and 1128 and 1051cm^{-1} in ***C2***.

FT-Raman vibrational patterns have very slight variations compared to FT-IR. The P=O stretching vibrations were observed at 1307 and 1273 cm^{-1} in ***L*** while shift to 1342 and 1290 cm^{-1} in ***C1*** and 1298 and 1219 cm^{-1} in ***C2***. FT-IR and FT-Raman vibrational patterns of ***L***, ***C1*** and ***C2*** are presented in **Figure S1** and **S2** of Supporting Information.

According to experimental section, the integrated intensities of ^{1}H NMR signals of the ligand ***L*** correspond to its structural formula; 6H in 7.47 ppm refers to ortho and para position, and 4H in 7.71 ppm refers to meta position. In ^{31}P NMR, the chemical shift is affected by the solvent, giving δ = 24.2 ppm in $CDCl_3$ and δ = 23.4 ppm in DMSO.

The integrated intensities of ^{1}H NMR signals of the complex ***C1*** correspond to its structural formula (1:1, mole ratio of ligand to tin reactant compound). The peak of ^{119}Sn NMR is appeared at -61 ppm, falling in the range of four-coordinate tin(IV) compounds. It seems that the binding of ligand is apparently different in the solution and in the crystal state and the ligand functions as monodentate. Similar to what was mentioned earlier about that phosphorus-based tin complexes [15-18], there are probably fast transactions in the solution and different types of five-coordinate and four-coordinate tin are in balance. In comparison with the ligand, ^{31}PNMR spectrum of the complex ***C1*** shows two peaks: one with the chemical displacement similar to the free ligand (24.4 ppm) and the other with an approximate difference of 9 ppm (33.4 ppm). Obtaining more information about these types requires the study of ^{31}P NMR at various temperatures, which, unfortunately, was not easily possible.

^{31}P NMR spectrum of the complex ***C2*** shows also two peaks: one with the chemical displacement similar to the free ligand (23.2 ppm) and the other with an approximate difference of 11 ppm (34.6 ppm).

For more accurate studies, computational methods were used to interpret the data. A fragment of crystal structure ***C1*** and ***C2*** complexes, including two metal centers and three bridging ligands was extracted from X-ray atomic coordinates and fully optimized in the solvent and gas phases using the relativistic effective core potential standard basis set LANL2DZ for metal atoms (Sn and Cu) and 6-311G(d) for the other atoms. The solvents used in the calculations include chloroform solvent for ***C1*** and DMSO solvent for ***C2*** (exactly the same conditions used in NMR spectra).

Interestingly, the optimized structure of the ***C1*** complex confirms the proposed four-coordinate type in solution ($Ph_2P(O)O$-$SnPh_3$), and it shows two different Sn-O interactions: 2.142 and 2.112 Å (in covalent range) and 2.269 and 2.325 Å (in coordination range) in the

chloroform solvent and gas phases respectively (**Figures 1** and **S3** of Supporting Information).

Similarly for ***C2***, two different Cu-O interactions are observed (**Figures 1** and **S3** of Supporting Information). Interactions in covalent range (1.939 and 1.914Å) and two interactions within the coordinated range (2.067 and 1.976Å), in the DMSO solvent and gas phases respectively.

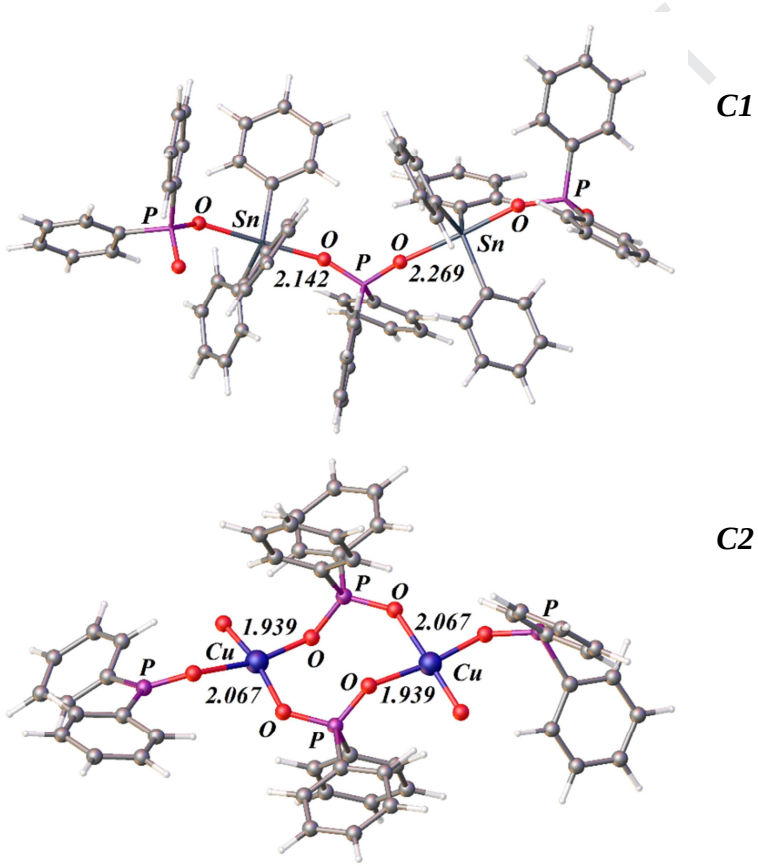

Fig. 1. Optimized structure of a fragment of coordination polymer ***C1*** and ***C2*** in solvent phase.

3.2 Description of Crystal Structures

All three compounds ***L***, ***C1*** and ***C2*** crystallized in a monoclinic crystal system with $P2_1/c$, $P2_1/n$ and $C2/c$ space group, respectively (Table 1). Selected bond lengths and angles are listed in Table 2 and hydrogen bonding data in Table 3.

Table 2. Selected bond distances (Å) and angles (°) for ***L***, ***C1***, and ***C2***.

Compound	*Bond length* (Å)	*Bond angles*(°)

L	P(1)-O(1)	1.505(10)	O(1)-P(1)-O(2)	116.54(6)
	P(1)-O(2)	1.550(10)	O(1)-P(1)-C(1)	110.43(6)
	P(1)-C(1)	1.794(13)	O(2)-P(1)-C(1)	102.92(6)
	P(1)-C(7)	1.798(13)	O(1)-P(1)-C(7)	111.01(6)
			O(2)-P(1)-C(7)	107.33(6)
			C(1)-P(1)-C(7)	108.05(6)
C1	Sn(1)-C(1)	2.122(14)	O(2)#1-Sn(1)-O(1)	174.57(4)
	Sn(1)-C(7)	2.122(14)	C(1)-Sn(1)-C(7)	124.31(6)
	Sn(1)-C(13)	2.135(14)	C(1)-Sn(1)-C(13)	119.38(6)
	Sn(1)-O(2)#1	2.225(10)	C(7)-Sn(1)-C(13)	116.25(5)
	Sn(1)-O(1)	2.238(10)	C(1)-Sn(1)-O(2)#1	83.52(5)
	P(1)-O(2)	1.514(10)	C(7)-Sn(1)-O(2)#1	92.32(5)
	P(1)-O(1)	1.516(10)	C(13)-Sn(1)-O(2)#1	92.22(5)
	P(1)-C(19)	1.803(14)	C(1)-Sn(1)-O(1)	91.09(5)
	P(1)-C(25)	1.810(15)	C(7)-Sn(1)-O(1)	91.32(5)
			C(13)-Sn(1)-O(1)	89.79(5)
C2	Cu(1)-O(1)	1.925(16)	O(1)-Cu(1)-O(1)	180.0(5)
	Cu(1)-O(1)	1.925(16)	O(1)-Cu(1)-O(2)	88.83(7)
	Cu(1)-O(2)	1.919(16)	O(1)-Cu(1)-O(2)	91.17(7)
	Cu(1)-O(2)	1.919(16)	O(1)-Cu(1)-O(2)	91.17(7)
	P(1)-O(1)	1.505(18)	O(1)-Cu(1)-O(2)	88.83(7)
	P(1)-O(2)	1.515(16)	O(2)-Cu(1)-O(2)	180.0(5)
	P(1)-C(1)a	1.827(5)		
	P(1)-C(1)	1.783(5)		
	P(1)-C(1)c	1.829(3)		
	P(1)-C(1)d	1.781(3)		

*3.2.1 Crystal structure of ligand **L***

Previously, the crystal structure of diphenylphosphinic acid (***L***) reported at different temperatures [19-22], and in this study, the crystal structure of ***L*** has been determined at 100 °K. Crystal data for the diphenylphosphonic acid in different temperature are listed in Table S1 of Supporting Information. The important point is that temperature variations do not have much effect on the structure, and in all literature diphenylphosphonic acid crystallized in a monoclinic crystal system with *P21/c* space group (Table **S1**).

In this study, the structure of diphenylphosphonic acid was investigated in a different interpretation. The geometry of phosphorus is tetrahedral and the lengths of P-O bonds are 1.505(10) and 1.550(10) Å respectively. O-H groups engage in intermolecular hydrogen bond with the adjacent P=O unit and create a chain along *b*-axis. Moreover, the phosphoryl oxygen, in another hydrogen interaction, is involved with phenyl ring, resulting in the 2D aggregation of molecules. Finally, weak bonds C5…C5 (3.337(3) Å) develop a crystal network in the third dimension (*a*-axis) (The structures of ***L*** are shown in **Figures 2** and **3**). In

comparison with hydrogen bonding pattern of ***L***, benzoic acid and its derivatives are present as binary accumulations and intermolecular hydrogen bonds result in the formation of six membered rings. (**Figure 4**).

Table 3. Hydrogen bond data for compound ***L*** (distances in Å and angles in °).

D-H...A	*d*(D-H)	*d*(H...A)	*d*(D...A)	<(DHA)	Symm. code
O(2)-H(2O)...O(1)#1	0.95	1.53	2.478(14)	174	#1 -x+1,y-1/2,-z+1/2
C(10)-H(10A)…O(1)	0.95	2.61	3.395(19)	140	x+1,y-3/2,-z+2

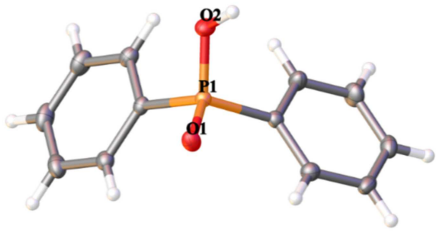

Fig. 2. Molecule of ***L*** with displacement ellipsoids at 50% probability.

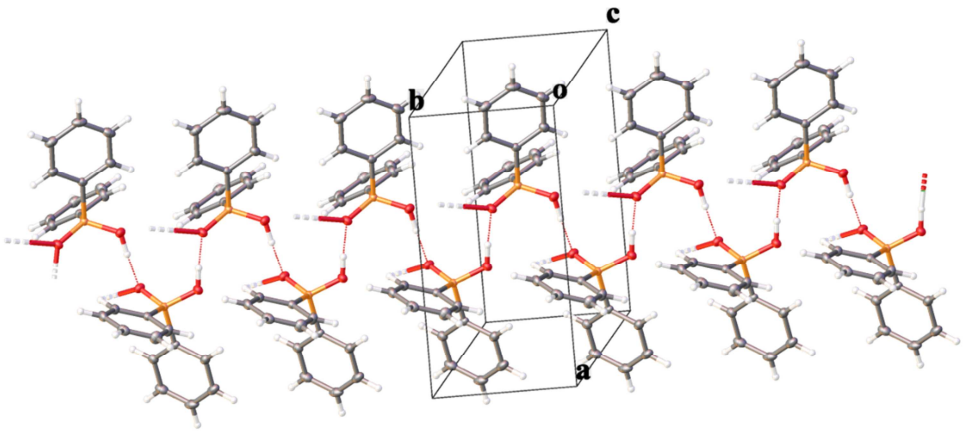

(a)

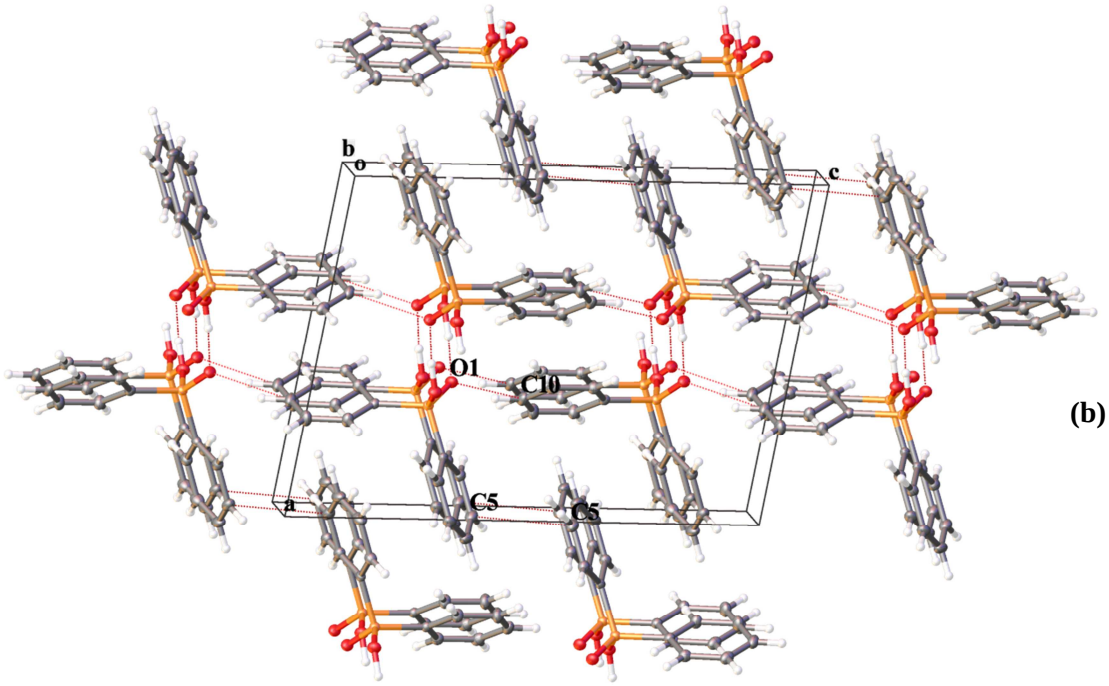

Fig. 3 1D polymeric chains along *c*-axis, showing intermolecular hydrogen bonds (a), and crystal packing fragment of ***L*** (b).

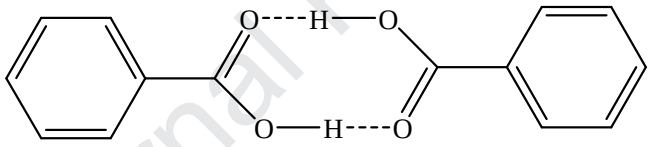

Fig. 4 Hydrogen bonding pattern in the structure of benzoic acid and its derivatives.

*3.2.2 Crystal structure of complex **C1***

In crystal structure of ***C1***, tin centers are connected by bidentate ligand ***L***, creating chains along the *b*-axis. The distance between the two centers of Sn is 6.341(19) Å. Sn(IV) centers have distorted trigonal bipyramidal coordination geometry with oxygen atoms at the axial positions and phenyl groups on equatorial planes. The *trans* angle around the tin atom is 174.57(4) º and the angles of C—Sn—C in belt position are 116.25(5)-124.31(6) º. The different bond lengths of Sn—O [2.225(10) and 2.238(10) Å] and also different angles of P—O—Sn (145.79(6) and 141.98(6) º, respectively) show that the bridging ligand is asymmetrically coordinated to metal centers. It seems that a more suitable interaction angle

has resulted in a better orbital overlap and a shorter bond. Beside, elongation of P—O bond in ***C1*** is simply attributed to the polarization of phosphoryl in the electrostatic field of Sn(IV).

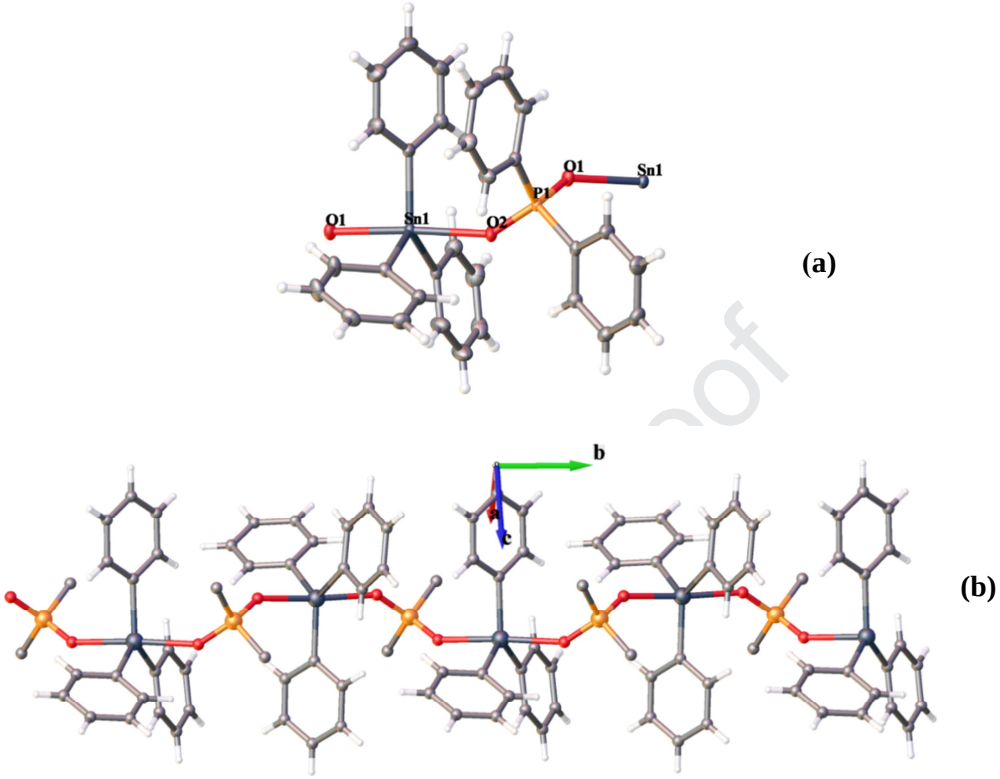

Fig. 5 Molecule of ***C1*** with displacement ellipsoids drawn at 50% probability level (a), A chain of molecules of ***C1*** bridged by tin. Phenyl groups on the ligand have been omitted for clarity (b).

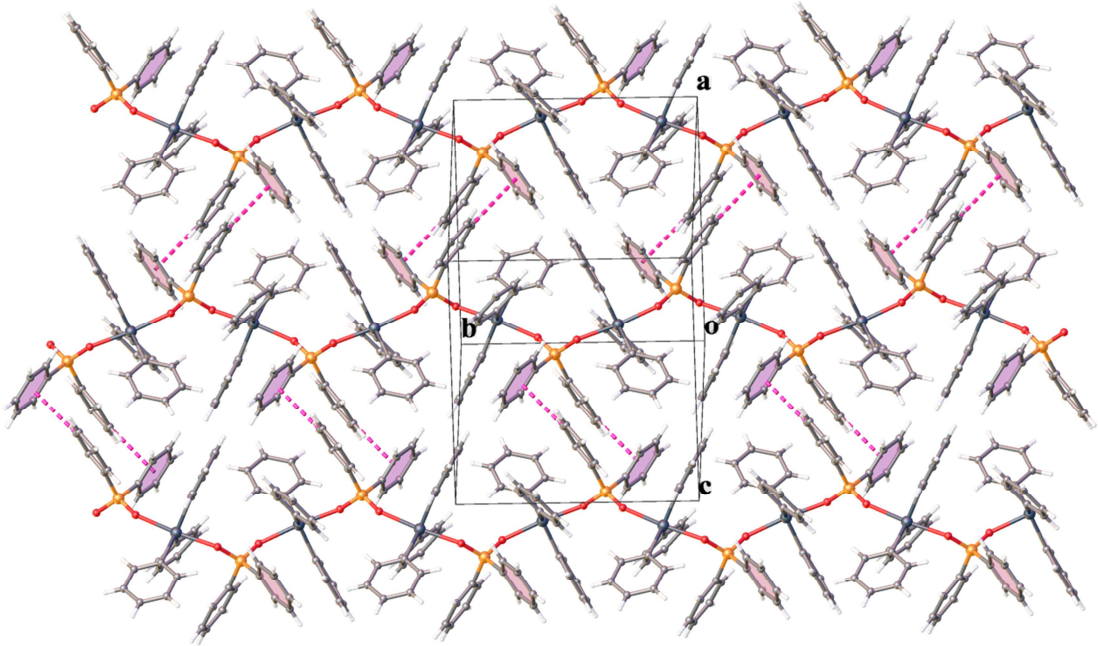

Fig. 6 A two-dimensional zigzag polymeric network of **C1** formed by CH–π intermolecular interactions **.**

As mentioned earlier, coordination interactions of Sn—O play an essential role in the formation and stability of supramolecular ***C1***. Adjacent coordination polymers are connected to two-dimensional networks (**Figures 5-6**) through CH…π interactions between the phenyl rings of ligands [C10–H10…Cg (Cg: the center of gravity of ligand phenyl ring): θ=161.36°, d(C23…Cg)=3.469(7) Å, d(H23…Cg)=2.535 Å]. These layers are also stabilized by weaker interactions H…H.

*3.2.3 Crystal structure of complex **C2***

The structure of ***C2*** comprises [010] chain motifs in which Cu atoms separated 5.053 Å are linked by two bridging phosphinate ligands. Copper has a square planar coordination with four O atoms each from four different phosphinates. The Cu—O bond lengths are in the range 1.919(16) – 1.925(16) Å, showing that the bridging ligand is asymmetrically coordinated to metal centers. The *trans*-O—Cu—O bond angles are 180.0(5), while the *cis*-O—Cu—O angles range from 88.83(7) to 91.17(7). Selected list of bond lengths and angles involving the Cu(II) centers is given in Table 2.

Adjacent 1D coordination polymers are connected through the CH…π interaction between the phenyl rings of ligands [C3d–H1…Cg and C4d–H1…Cg (Cg: the center of gravity of ligand phenyl ring): d(C3d–H1…Cg)=3.328 Å, d(C4d–H1…Cg)=3.626 Å]. As a result of these interactions, two-dimensional networks are formed in the structure. Weaker interactions of H…H stabilize the structure by connecting the two-dimensional layers into a 3D network. (The structures of ***C2*** are presented in **Figures 7** and **8**).

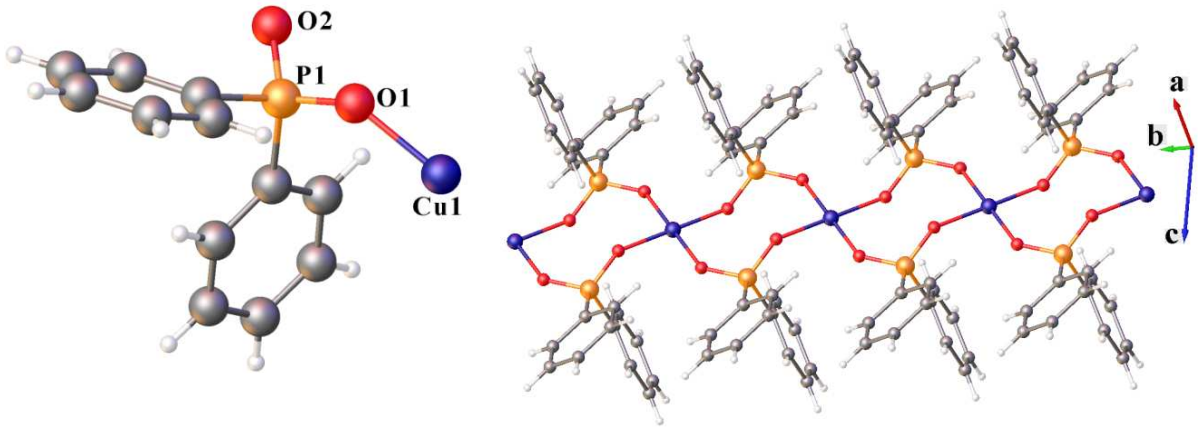

(a) **(b)**

Fig. 7 (a) A molecule of ***C2*** with displacement ellipsoids drawn at the 50% probability level, (b) The coordination chain of ***C2*** extended along *b*.

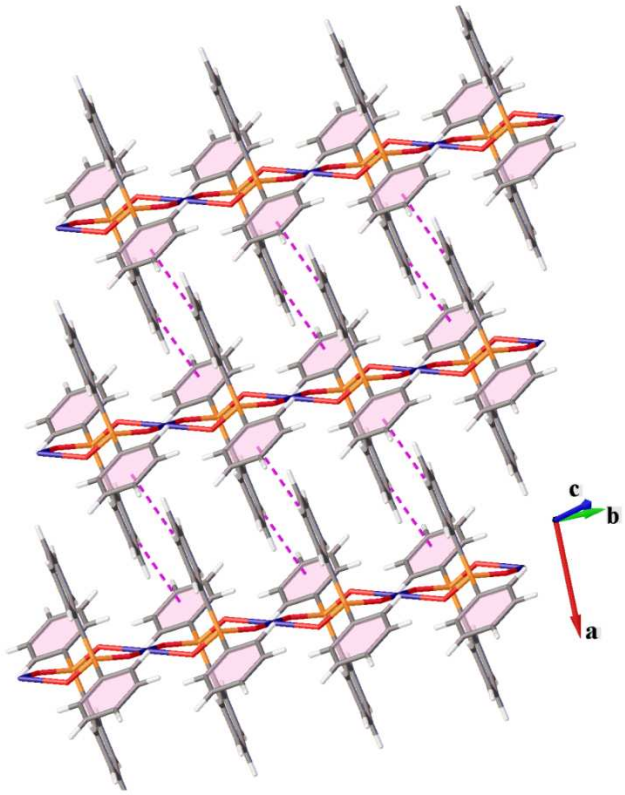

Fig. 8 CH–π interactions in ***C2***, connecting the coordination chains in a 2D network.

3.3 Hirsfeld surface analysis

The Hirshfeld surfaces and associated fingerprint plots were performed using Crystal Explorer 3.1 [23]. The derivation of Hirshfeld surfaces and their breakdown of the corresponding 2D fingerprint plots [24] provide a convenient mean of quantifying the interactions within the crystal structures, revealing significant similarities and differences

between related structures. The sharp spikes of the fingerprint plots represent their importance in the formation of a given crystal structure and also provide a platform for the evaluation of the contribution of different atom....atom contacts which contribute to the packing. It should be noted that after reading CIF into the Crystal Explorer program, all bond lengths to hydrogen are automatically modified to typical standard neutron values (C-H = 1.083 Å, N-H = 1.009 Å and O-H = 0.983 Å) [25]. **Figure 9** shows the Hirshfeld surfaces and fingerprint plots of the three title compounds ***L***, ***C1*** and ***C2***. Hirshfeld surfaces were generated using a high (standard) surface resolution. The 3-D d_{norm} surfaces were mapped by using a fixed color scale of 0.76 (red) to 2.4 (blue) over d_{norm} ranges –0.864 to 1.217Å for ***L***, range –0.777 to 1.392Å for ***C1***, and –0.682 to 1.239Å for ***C2***, respectively. The 2-D fingerprint plots were displayed by using the standard 0.6-2.8 Å view with the de and di distance scales displayed on the graph axes. Two sharp spikes in ***L*** imply to O···H hydrogen bond, and in ***C1*** and ***C2*** sharp spikes represent Sn...O and Cu...O contacts. According to **Figure 9**, the Hirshfeld surfaces of ***L***, ***C1*** and ***C2*** contain relatively large red circles (label "a") corresponding H…O=P hydrogen bonds between the hydroxyl and phosphoryl groups from two adjacent molecules of ***L***, or. Sn...O and Cu...O bonds in ***C1*** and ***C2***. Lighter and smaller red circles (label "b") in ***C2*** belong to either CH···π contacts.

The Quantitative measures of the Hirshfeld surface for molecules ***L***, ***C1***, and ***C2*** are presented in Table 4. The lowest Hirshfeld volume and surface area of ***L*** indicates that this molecule has a more crowded environment than the other molecules, and this feature is also apparent in the fingerprint plot by the compact pattern of this molecule.

The globularity is a quantity measuring the extent the surface area varies from that of a sphere, being 1.0 for a sphere, the molecule of ***L*** has a maximum amount of globularity as a result of the most convex character of its surface. Also, asphericity is highest for ***L***, which shows more ablations of these surfaces. According to the Table 4, the largest volume and

surface area and the lowest of globularity and asphericity are shown for ***C1***, caused by three phenyl groups bound to tin.

Table 4. Quantitative measures of Hirshfeld surface for ***L, C1*** and ***C2***.

Compound	Molecular volume (Å^3)	surface area (Å^2)	Globularity of the surface	Asphericity
L	255.17	245.44	0.793	0.125
C1	612.41	485.46	0.718	0.022
C2	266.53	258.27	0.776	0.113

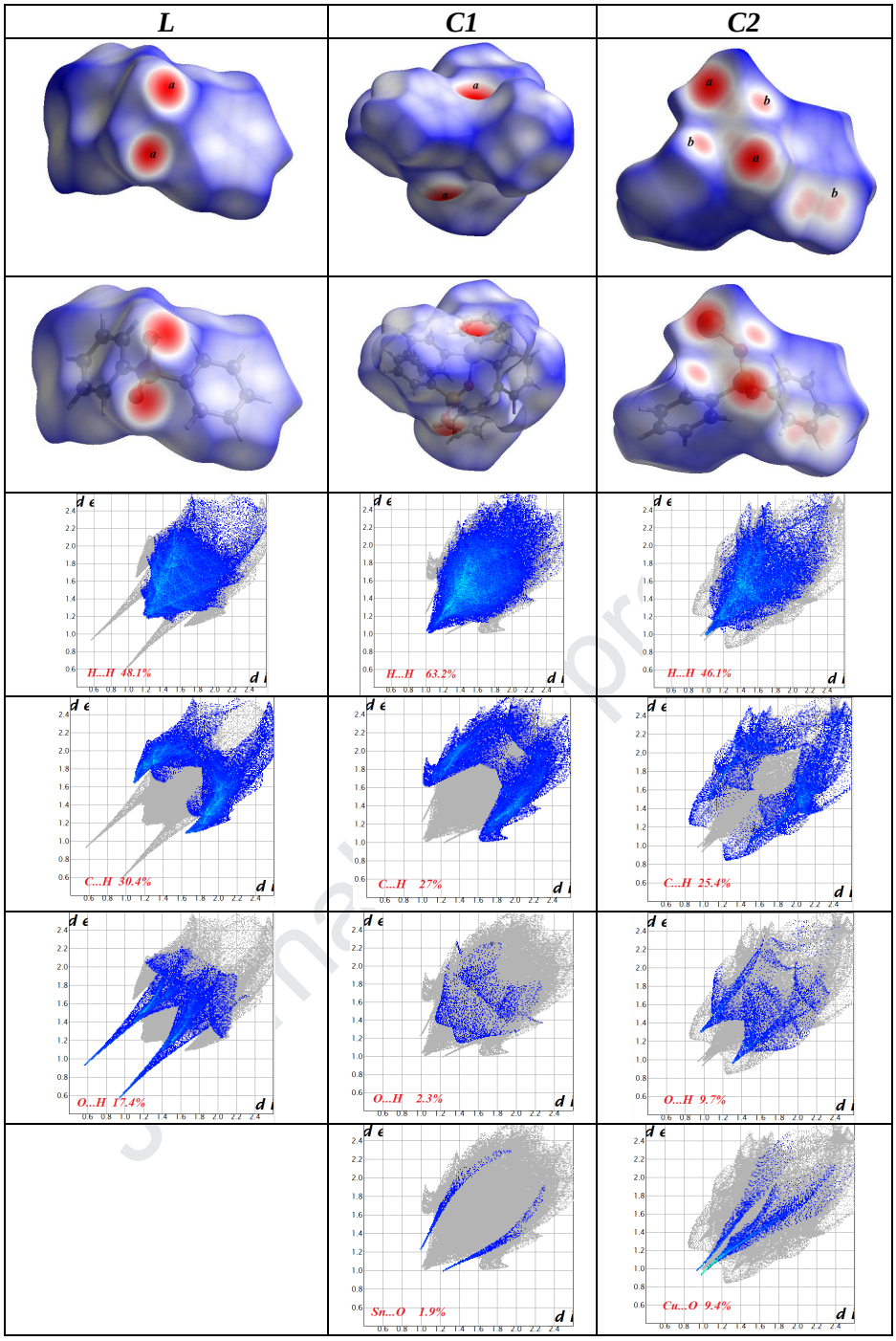

Fig. 9 Hirshfeld surfaces mapped with d_{norm} function and fingerprint plots for ***L***, ***C1*** and ***C2***

The relative contributions of particular intermolecular interactions are presented as a chart in **Figure10**. The H···H interaction dominates in crystal packing, followed by C···H contacts of CH···π interactions. The O···H interaction is largest for the ***L*** molecule.

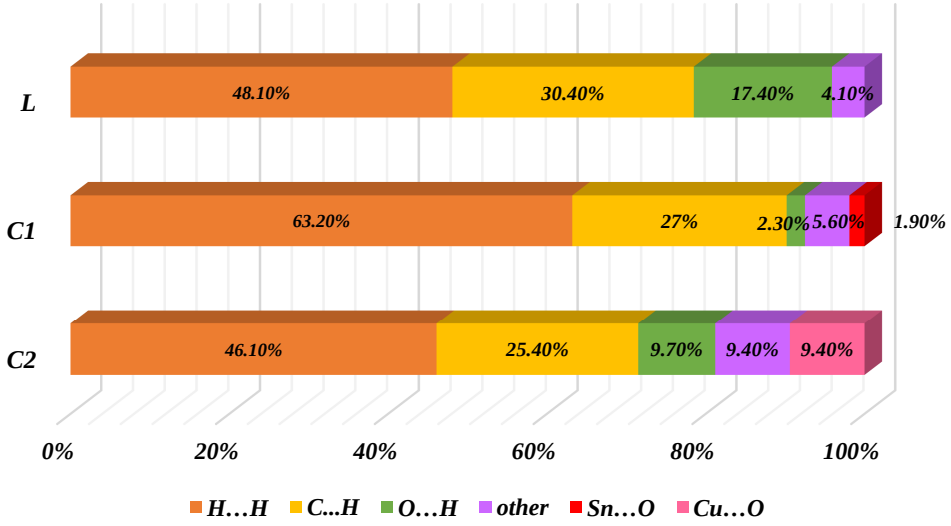

Fig. 10 Relative contribution of various atom…atom contacts contributing towards the crystal packing of the ***L***, ***C1*** and ***C2***.

4 Conclusions

In summary, we reported the crystal structure of ligand (***L***) and its coordination polymers with tin and copper (***C1*** and ***C2***). The X-ray results reveal that the crystal structure of ***L*** is mainly governed by chains of O-H…O=P hydrogen bonds, which is a different pattern compared to the similar compound of benzoic acid with H-bonded ring motifs. The deprotonated ligand functions in a bridging mode in both complexes, generating coordination chain motifs. In ***C1*** structure, Sn(IV) centers are five-coordinate and have distorted trigonal bipyramidal geometry while in the case of ***C2***, adjacent copper atoms are double-bridged by two ligands and the geometry of the copper atom has a square planar configuration. The metal-contributed chains in ***C1*** and ***C2*** are connected by C–H…π and H…H interactions to construct the crystal packing networks. The molecular Hirshfeld surface and 2D fingerprint plots were used for quantitative mapping of these interactions. The chemical behavior of the complexes in the solution is different from the solid state structures, confirmed by the calculated in the solvent and gas phase structures. It seems that the binding of the ligand is different in the soluble state than in the crystal structure; monodentate in the solvent and

bidentate in solid-state. Sn NMR spectrum in solution suggests an exchange between coordination compounds and dissociated species, at ambient temperature.

Acknowledgement

The financial supports of this work was provided by Tarbiat Modares University, Iran National Science Foundation (INSF) Tehran, Iran and by the Research Branch, Islamic Azad University, Tehran, Iran. The crystallographic part was supported by the project 18-10438S of the Czech Science Foundation using instruments of the ASTRA lab established within the Operation program Prague Competitiveness - project CZ.2.16/3.1.00/24510.

References

[1] A. U. Czaja, N. Trukhan, U. Muller, Industrial applications of metal–organic frameworks, Chem. Soc. Rev. 38 (2009) 1284– 1293.

[2] H. Furukawa, K. E. Cordova, M. O'Keeffe, O. M. Yaghi, The chemistry and applications of metal-organic frameworks. Science, 341 (2013). 974.

[3] M. Dincˇa, J. R. Long, Hydrogen Storage in Microporous Metal–Organic Frameworks with Exposed Metal Sites. Angew. Chem. Int. Ed. 47 (2008) 6766–6779.

[4] G. K. H. Shimizu, R. Vaidhyanathan, J. M. Taylor, Phosphonate and sulfonate metal organic frameworks, Chem. Soc. Rev. 38 (2009) 1430–1449.

[5] T. S. Basu Baul, D. Dutta, A. Duthie, N. Guchhait, B. G. M. Rocha, M. F. C. Guedes da Silva, R. B Mokhamatam,.N. Raviprakash, S. K. Manna, New dibutyltin(IV) ladders: Syntheses, structures and, optimization and evaluation of cytotoxic potential employing A375 (melanoma) and HCT116 (colon carcinoma) cell lines in vitro, J. Inorg. Biochem., 166 (2017) 34-48

[6] S. Shahzadi, S. Ali, K. Shahid, M. Yousaf , S. K. Sharma, K. Qanungo, Interaction of Di- and Triorganotin(IV) Compounds with Carboxylate Ligand: Synthesis, Spectral

Characterization, Semi-Empirical Study and In Vitro Antimicrobial Activities, J. Chin. Chem. Soc., 57 (2010) 659-670

[7] D.L. Reger, A. Debreczeni, M.D. Smith, J. Jezierska, A. Ozarowski, Copper(II) Carboxylate Dimers Prepared from Ligands Designed to Form a Robust π···π Stacking Synthon: Supramolecular Structures and Molecular Properties, Inorg. Chem., 51 (2012) 1068–1083

[8] A.N. Wein, R. Cordeiro, N. Owens, H. Olivier, K. I. Hardcastle, J. F. Eichler, Synthesis and characterization of Cu(II) paddlewheel complexes possessing fluorinated carboxylate ligands, Journal of Fluorine Chemistry, 130(2009) 197-203

[9] T. Aiyelabol, E. Akinkunmi, E. Obuotor, I. Olawuni, D. Isabirye, J. Jordaan, Synthesis Characterization and Biological Activities of Coordination Compounds of 4-Hydroxy-3-nitro-2 H -chromen-2-one and Its Aminoethanoic Acid and Pyrrolidine-2-carboxylic Acid Mixed Ligand Complexes, Bioinorg Chem Appl., 9 (2017)1-9.DOI: 10.1155/2017/6426747

[10] For C1: Bruker, Programs APEX II, version 2.0-1; SAINT, version 7.23A, For C2: Bruker (2005). APEX2 software package, Bruker AXS Inc., 5465, East Cheryl Parkway, Madison, WI 5317.

[11] A.D. Becke, Density-functional thermochemistry. III. The role of exact exchange, J. Chem. Phys. 98 (1993) 5648-5652.

[12] M.J. Frisch, G.W. Trucks, H.B. Schlegel, G.E. Scuseria, M.A. Robb, J.R. Cheeseman, G. Scalmani, V. Barone, B. Mennucci, G.A. Petersson, H. Nakatsuji, M. Caricato, X. Li, H.P. Hratchian, A.F. Izmaylov, J. Bloino, G. Zheng, J.L. Sonnenberg, M. Hada, M. Ehara, K. Toyota, R. Fukuda, J. Hasegawa, M. Ishida, T. Nakajima, Y. Honda, O. Kitao, H. Nakai, T. Vreven, J.A. Montgomery Jr., J.E. Peralta, F. Ogliaro, M. Bearpark, J.J. Heyd, E.

Brothers, K.N. Kudin, V.N. Staroverov, T. Keith, R. Kobayashi, J. Normand, K. Raghavachari, A. Rendell, J.C. Burant, S.S. Iyengar, J. Tomasi, M. Cossi, N. Rega, J.M. Millam, M. Klene, J.E. Knox, J.B. Cross, V. Bakken, C. Adamo, J. Jaramillo, R. Gomperts, R.E. Stratmann, O. Yazyev, A.J. Austin, R. Cammi, C. Pomelli, J.W. Ochterski, R.L. Martin, K. Morokuma, V.G. Zakrzewski, G.A. Voth, P. Salvador, J.J. Dannenberg, S. Dapprich, A.D. Daniels, O. Farkas, J.B. Foresman, J.V. Ortiz, J. Cioslowski, D.J. Fox, Gaussian 09, Revision D.01, Gaussian, Inc., Wallingford CT, 2013.

[13] C.T. Lee, W.T. Yang, R.G. Parr, Phys. Rev. B 37 (1988) 785-789.

[14] P.J. Hay, W.R. Wadt, J. Chem. Phys. 82 (1985) 299-310.

[15] K. Gholivand, A. Gholami, S. K. Tizhoush, K. J. Schenk, F. Fadaei, A. Bahrami, Steric and electronic control over the structural diversity of N-(n-pyridinyl) diphenylphosphinicamides (n ¼ 2 and 4) as difunctional ligands in triphenyltin(IV) adducts, RSC Adv, 4.(2014) 44509- 44516.

[16] K. Gholivand, A. Gholami, A. A. V. Ebrahimi, S. T. Abolghasemi, M. D. Esrafili, F. T. Fadaei, K. J. Schenk, Triphenyltin(IV) adducts of diphosphoryl ligands: structural, electronic and energy aspects from X-ray crystallography and theoretical calculations, RSC Adv., 5 (2015) 17482-17492.

[17] K. Gholivand, A. Gholami, K. J. Schenk, M. D. Esrafili, K. Farshadfar, Supramolecular assemblies of organotin(IV)diphosphoryl adducts: Insights from X-rays and DFT. RSC Adv., 5 (2015), 98610-98617.

[18] K. Gholivand, A. A. EbrahimiValmoozi, A. Gholami, M. Dusek, V. Eigner, S. Abolghasemi, Synthesis, characterization, crystal structures, QSAR study and antibacterial activities of organotin bisphosphoramidates. J. Organomet. Chem., 806, 15 (2016) 33-44.

[19] D. Fenske, R Mattes, J. Löns, K. F. Tebbe, Die Kristallstruktur von Diphenylphosphinsaure, Chem. Ber. 106 (1973) 1139-1144

[20] G. Siasios and E. R. T. Tiekink, Crystal structure of diphenylphosphinic acid (redetermination at 173 K), $C_{12}H_{11}O_2P$, Zeitschrift für Kristallographie 209 (1994) 547.

[21] K. A. Lyssenko, G. V. Grintselev-Knyazev, M. Yu. Antipin, Nature of the P–O bond in diphenylphosphonic acid: experimental charge density and electron localization function analysis, Mendeleev Commun., 12(4) (2002) 128–130.

[22] W. Gao, B. Shi, Crystal Structure of Diphenylphosphinic Acid, Mol. Cryst. Liq. Cryst., 623(2015)305–309.

[23] S. K. Wolff, D. J. Grimwood, J. J. McKinnon, M. J. Turner, D. Jayatilaka and M. A. Spackman, CrystalExplorer, version 3.0; University of Western Australia: Crawley, Australia, 2012.

[24] M. A. Spackman and J. J. McKinnon, CrystEngComm, 2002, 4, 378

[25] F. H. Allen, O. Kennard, D. G Watson, L. Brammer, A. G. Orpen, R. Taylor, Tables of Bond Lengths determined by X-Ray and Neutron Diffraction. Part 1. Bond Lengths in Organic Compounds. Journal of the Chemical Society, Perkin Transactions, 2 (1987) S1-S19. http://dx.doi.org/10.1039/p298700000s1

Highlights

- Synthesis and characterization of a phosphinic acid ligand and its two polymeric complexes.
- The structural motifs in the complexes are linked by M—O—P—O—M bonds."
- The chemical behavior of the complexes in the solution is different from the solid state structures.

Editor-in-Chief of *Journal of Molecular Structure*

Dear Prof. Rui Fausto

Wishing you a pleasant time, it is a great honor for me to have the opportunity of writing to you. My co-authors and I are submitting a revised manuscript entitled: "**Synthesis and structural characterization of phosphinate coordination polymers with tin(IV) and copper(II)**", by Khodayar Gholivand, Nasrin Fallah, Ali Asghar Ebrahimi, Akram Gholami, Michal Dusek, Vaclav Eigner, Mahsa Pooyan, Fahimeh Mohammadpanah for possible publication in one of the forthcoming volumes of *J. Mol. Stru.* The article is original and unpublished and is not being considered for publication elsewhere. I also confirm that all co-authors are aware of its content, approve its submission, and certify that the article has not been published previously and is not under consideration for publication elsewhere. Also, no conflict of interest exists and the authors declare no competing financial interest.

Yours sincerely,
Khodayar Gholivand, Ph.D.
Research Officer
Department of Chemistry-Faculty of Sciences
Tarbiat Modares University, P.O.Box: 14115-175
Phone: +98-21-82884422